Hong Kong J Radiol. 2024;27(2):e125-34. Published 13 Jun 2024 | https://doi.org/10.12809/hkjr2317714

PICTORIAL ESSAY

Radiologic-Pathologic Review of Non-Epithelial Malignancies and Metastases in the Breast: A Pictorial Essay

RYS Mak[1], AHC Wong[1], CKM Mo[1], KH Chin[1], JSC Wong[2], AYT Lai[1], WWC Wong[1]

[1]Department of Radiology, Pamela Youde Nethersole Eastern Hospital, Hong Kong SAR, China
[2]Department of Nuclear Medicine, Pamela Youde Nethersole Eastern Hospital, Hong Kong SAR, China

INTRODUCTION

Most malignant tumours in the breast are primary epithelial malignancies. Non-epithelial malignancies and metastases from other organs or tissues are rare. Many such malignancies have variable and non-specific radiological features and may resemble epithelial breast carcinomas or even benign breast lesions. Nevertheless, familiarity with their common imaging appearance is crucial for facilitating timely diagnosis and determining radiopathological concordance. This pictorial essay reviews the radiological appearance of important non-epithelial malignancies and metastases in the breast with histopathological correlation.

METASTASES TO THE BREAST

Metastases to the breasts from non-mammary primary tumours account for 0.5% to 2.0% of all breast malignancies.[1] The most common sources are melanoma; non-Hodgkin lymphoma; sarcoma; and carcinoma of the lung, stomach, ovaries, and kidney.[1] Clinically, metastases to the breast are generally not associated with chest wall fixation, *peau d'orange* appearance, Paget's disease of bone, skin retraction, nipple retraction, or discharge.[2] The lesions tend to be superficially located in the upper outer quadrant.[3]

The most common mammographic manifestations of metastases to the breast are one or more circumscribed upper outer quadrant masses (Figure 1) without spiculation or calcifications.[4] Another reported manifestation is a diffuse pattern resembling inflammatory breast carcinoma in cases of lymphatic metastases, most commonly from contralateral breast cancer, gastric, and ovarian carcinoma.[2,5]

Correspondence: *Dr RYS Mak, Department of Radiology, Pamela Youde Nethersole Eastern Hospital, Hong Kong SAR, China*
Email: mys877@ha.org.hk

Submitted: 25 March 2023; Accepted: 29 September 2023.

Contributors: RYSM, JSCW, AYTL and WWCW designed the study. RYSM, AHCW, CKMM, KHC and AYTL acquired the data. RYSM, AHCW, JSCW and AYTL drafted the manuscript. CKMM, KHC, AYTL and WWCW critically revised the manuscript for important intellectual content. All authors had full access to the data, contributed to the study, approved the final version for publication, and take responsibility for its accuracy and integrity.

Conflicts of Interest: All authors have disclosed no conflicts of interest.

Funding/Support: This study received no specific grant from any funding agency in the public, commercial, or not-for-profit sectors.

Data Availability: All data generated or analysed during the present study are available from the corresponding author on reasonable request.

Ethics Approval: The study was approved by the Hong Kong East Cluster Research Ethics Committee of Hospital Authority, Hong Kong (Ref No: HKECREC-2022-035). The requirement for patient consent was waived by the Committee due to the retrospective nature of the study.

Acknowledgement: The authors thank Dr KC Leung from the Department of Clinical Pathology of Pamela Youde Nethersole Eastern Hospital for critically revising the manuscript.

Declaration: Part of the manuscript was previously presented as a poster in the 30th Annual Scientific Meeting of the Hong Kong College of Radiologists (12-13 November 2022, virtual).

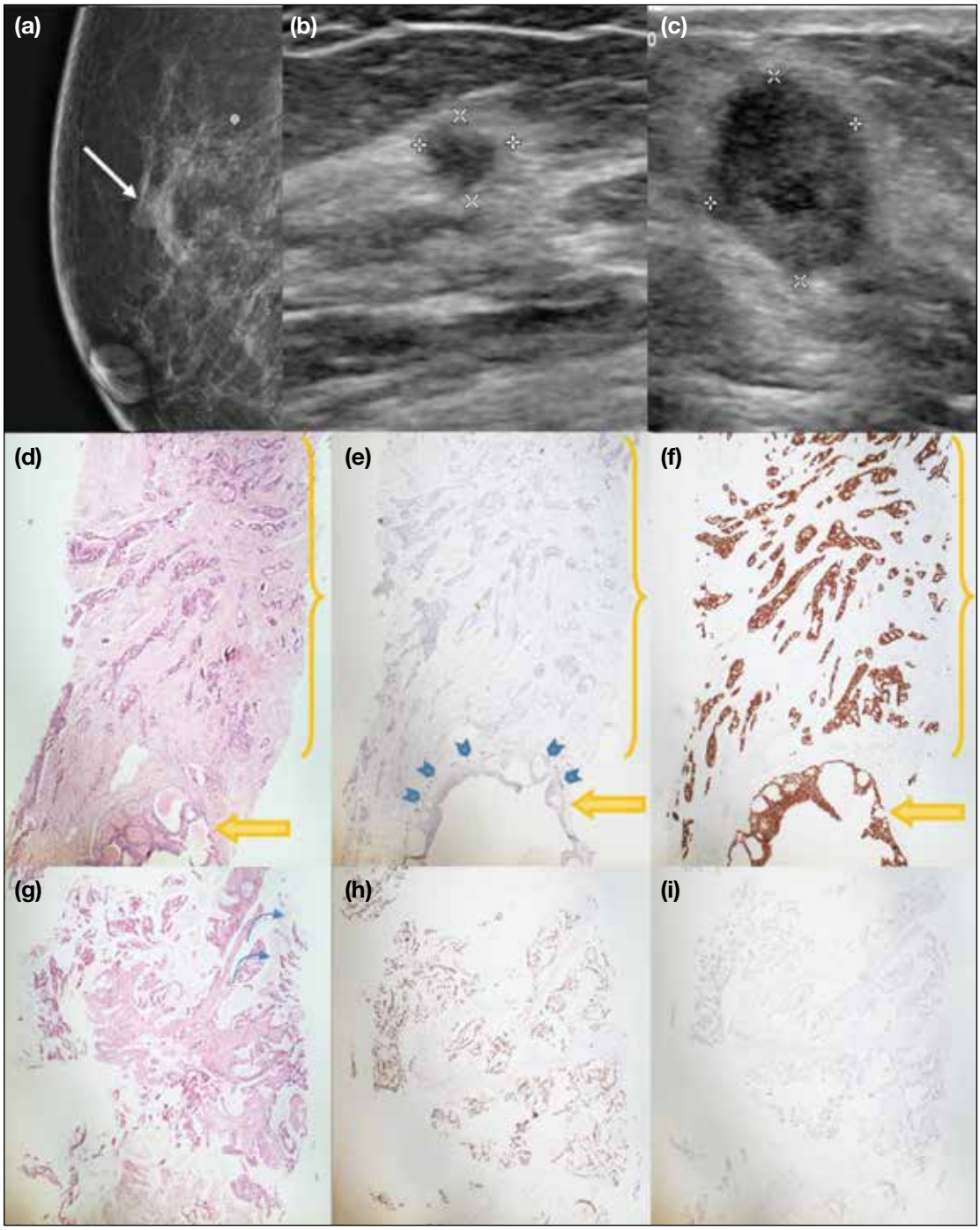

Figure 1. An 81-year-old woman with known carcinoma of the lung was found to have synchronous primary right breast invasive ductal carcinoma and a right axillary metastatic lesion from lung adenocarcinoma. (a) Mammogram showing an oval isodense mass in the upper outer quadrant of the right breast at anterior depth (arrow). (b) Ultrasound reveals a corresponding irregular hypoechoic mass in the upper outer quadrant of the right breast. (c) Another oval hypoechoic mass with non-parallel (taller-than-wide) orientation is seen in the right axillary subcutaneous region. (d-f) Low-power views (×4) of the right breast mass biopsy in haematoxylin and eosin (H&E) staining (d), p63 staining (e) and GATA binding protein 3 (GATA-3) staining (f) showing invasive ductal carcinoma (yellow brackets) featuring infiltrative nests and tubules. On immunohistochemistry (IHC), the tumour cells are diffusely positive for GATA-3, supportive of primary breast malignancy. A small component of ductal carcinoma in situ (yellow arrows) with preservation of the myoepithelial layer is highlighted by p63 staining (blue arrowheads in [e]). (g-i) Low-power views (×4) of the right axillary mass biopsy in H&E staining (g), thyroid transcription factor-1 (TTF-1) staining (h) and GATA-3 staining (i) showing fibroadipose tissue infiltrated by irregular glands, with some extracellular mucin pools in proximity (curved arrows in [g]). The morphology and IHC profile were similar to those of a specimen of prior lung carcinoma in the same patient (not shown). The tumour cells are diffusely positive for TTF-1 and negative for GATA-3. Overall findings are consistent with metastatic adenocarcinoma with mucinous features of a lung primary. Image courtesy of Dr KC Leung, Department of Clinical Pathology, Pamela Youde Nethersole Eastern Hospital, Hong Kong (d-i).

Sonographic findings are similarly non-specific; they can appear as solid masses that are circumscribed or ill-defined and hypo- or hyperechoic, with posterior shadowing or enhancement (Figure 1).[4,6]

Metastatic tumours can be recognised pathologically by their unusual histological patterns, lack of an in situ component, predominant periductal and/or perilobular distribution, and extensive lymphovascular involvement.[7] In addition, clinical history, comparison of the histology of mammary and extramammary tumours (if any), and use of immunohistochemical markers that are organ- or tumour-specific provide indispensable information for delineating the origin of the primary tumour (Figure 1).[7]

SARCOMA

Breast sarcomas are a group of aggressive tumours of mesenchymal origin accounting for <1% of all breast malignancies.[8] They can be primary, or secondary to previous radiotherapy for breast or intrathoracic malignancies.[8] Primary sarcomas occur predominantly in women, with the highest incidence in patients aged between 45 and 50 years, except for angiosarcomas, which tend to occur in younger women with a reported mean age of <40 years.[9,10] The most common subtypes of breast sarcomas are angiosarcomas, fibrosarcomas, and undifferentiated pleomorphic sarcomas.[9] Angiosarcomas have a worse prognosis than other types of breast sarcomas (Figures 2 and 3).[11]

On mammography, the most common finding is a solitary, oval, high-density mass with either indistinct or circumscribed margins and no calcifications (Figure 3).[10] However, coarse osteoid calcifications may occasionally be found in breast sarcomas with osteosarcoma features.[11,12]

On ultrasound, breast sarcomas typically appear as oval masses with indistinct margins, hypoechoic or complex echotexture, posterior acoustic shadowing, and internal vascularity (Figure 3).[10] Diffuse abnormal mixed hyper-and hypoechogenicity without a discrete mass has been reported in up to 38% of patients with breast angiosarcoma.[13] Hypervascularity on colour Doppler imaging is a typical feature of angiosarcoma; up to 54% of masses are hyperechoic or mixed hyper- and hypoechoic, which may also reflect the vascular nature of angiosarcoma.[13]

On magnetic resonance imaging, breast sarcoma typically appears as an oval irregular mass that is hypointense on T1-weighted images and hyperintense on T2-weighted images, with heterogeneous initial rapid enhancement, and washout curves (i.e., a relatively rapid uptake with reduction in enhancement towards the latter part of the study) or plateau curves (i.e., initial uptake followed by the plateau phase towards the latter part of the study) on dynamic imaging.[10]

LYMPHOMA

Breast lymphoma is a haematological neoplasm that originates in the lymphoid tissue of the breast and may be primary or secondary. Together, they

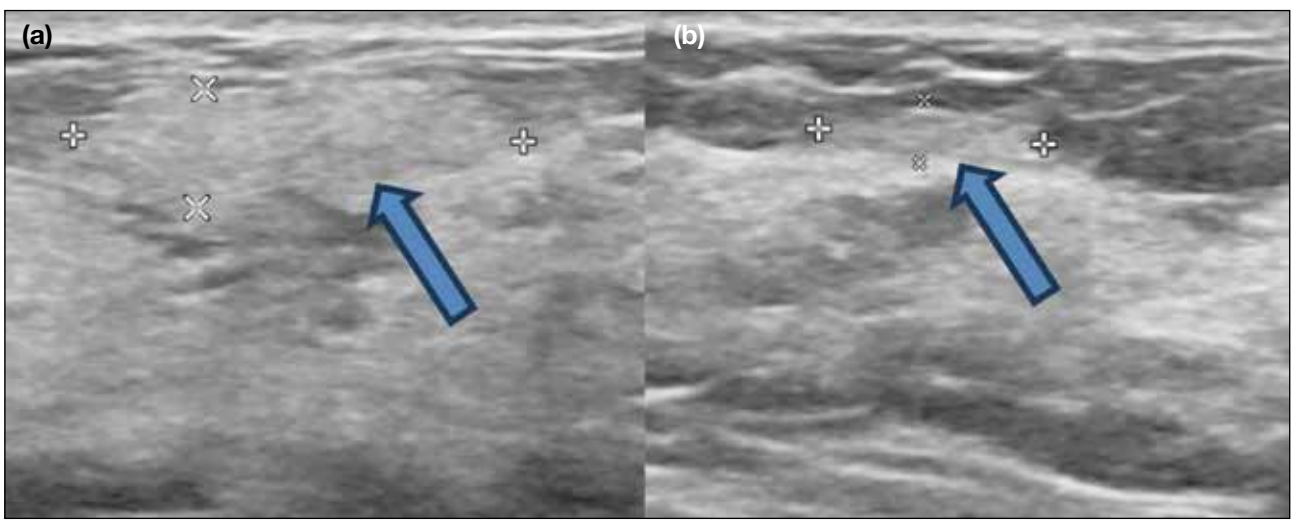

Figure 2. A 43-year-old woman first presented with lumpiness in the upper outer quadrant of the right breast. No suspicious mass or microcalcifications were seen on initial bilateral mammograms. Two oval, parallel echogenic lesions (arrows) with indistinct border were detected on ultrasound at the site indicated by the patient. Histopathology showed adipose tissue only. After 1 year, she returned with a rapidly enlarging mass in the upper outer quadrant of the right breast; the findings are shown in Figure 3.

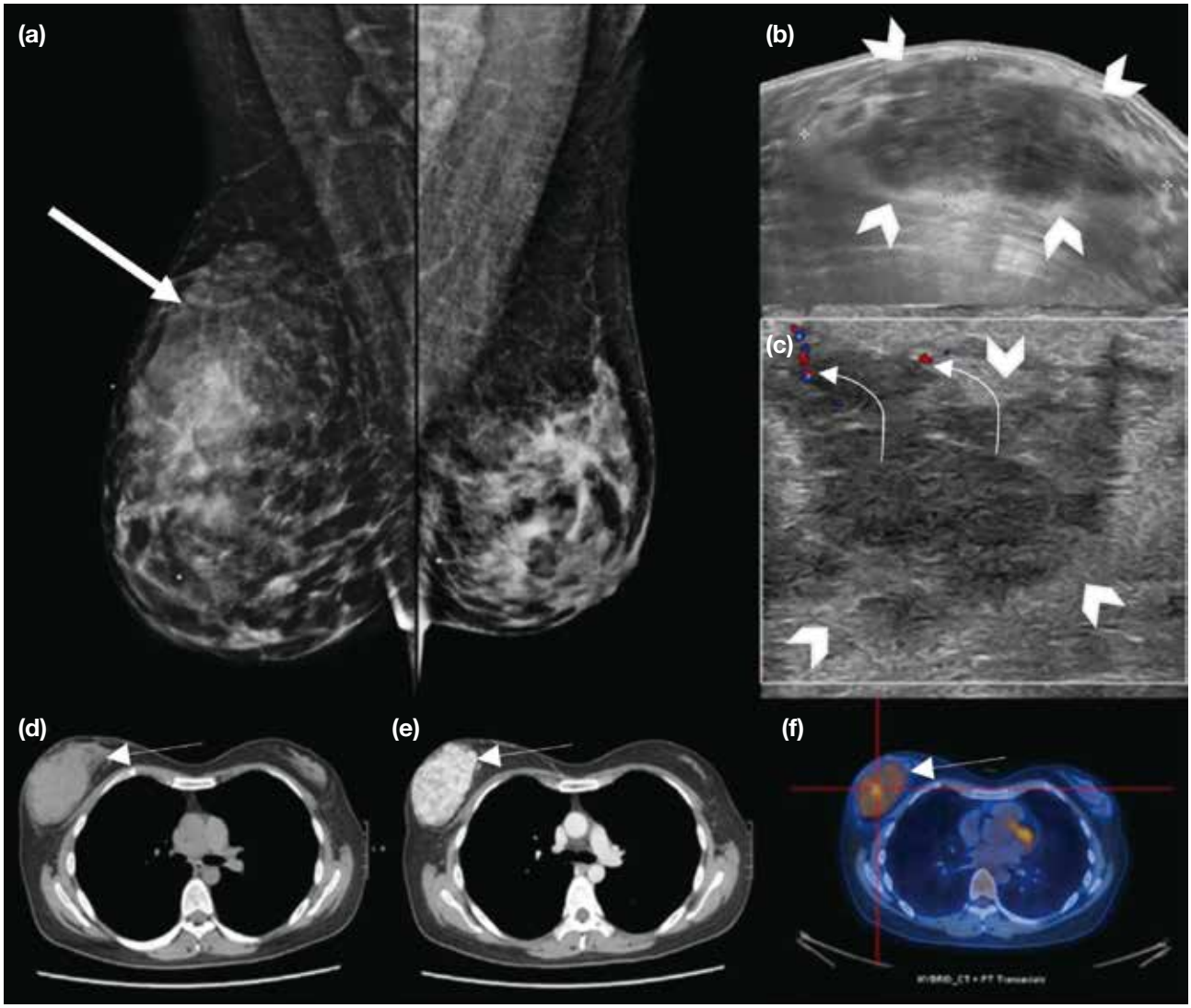

Figure 3. The same patient described in Figure 2 returned complaining of a rapidly enlarging right breast mass at 1 year after initial assessment. (a) The current bilateral mammograms in mediolateral oblique view shows a new iso- to hyperdense mass with obscured border occupying most of the upper outer quadrant of the right breast (thick arrow). (b, c) A large irregular heterogeneous mass (arrowheads) is seen in the upper outer quadrant of the right breast on ultrasound. Its periphery is mainly hyperechoic and blends in with the normal breast tissue. Minimal peripheral vascularity is noted (curved arrows in [c]). Staging contrast-enhanced computed tomography (d, e) and ^{18}F-fluorodeoxyglucose positron emission tomography/computed tomography (f) show a corresponding avidly enhancing hypermetabolic right breast mass (thin arrows) with no distant metastases. The histopathological diagnosis was angiosarcoma.

represent approximately 0.04% to 0.7% of all breast malignancies.[14] Primary breast lymphoma accounts for 0.85% to 2.2% of all extranodal malignant lymphomas, while secondary breast lymphoma is the most common malignancy with secondary involvement of the breast.[15,16] Breast lymphoma most commonly presents as a painless, enlarging, palpable mass.[15] Multiple masses are found in <10% of patients and bilateral involvement is found in approximately 10% of patients, although these findings are more commonly identified in secondary breast lymphoma cases.[15]

On mammography, breast lymphoma manifests as a solitary, non-calcified, oval or lobulated mass. It may have circumscribed or indistinct margins (Figure 4). Infiltrative patterns such as global asymmetry and trabecula and skin thickening are uncommon findings.[12] Skin thickening and lymphedema are reported in only up to 8% of patients (Figure 5).[17] Calcifications, architectural distortion, and spiculations are rare.[12]

Sonographic features of breast lymphoma are non-specific, appearing as an oval or irregular mass of hyper-,

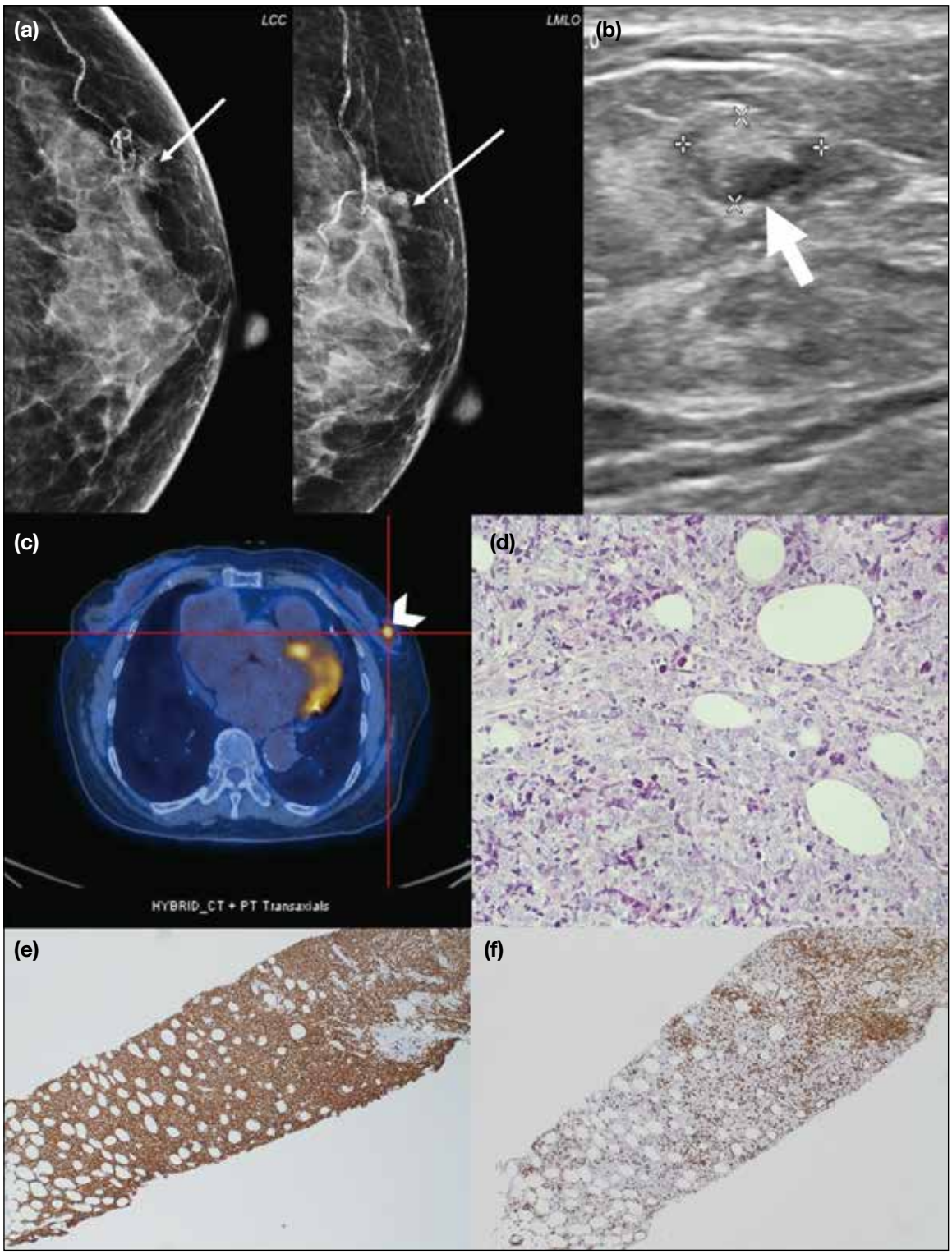

Figure 4. Primary diffuse large B-cell lymphoma presenting as a palpable left breast lump in an 88-year-old woman. (a) Cropped magnified views of left mammogram focusing on the upper outer quadrant showing an oval, circumscribed, equal density mass (thin arrows). (b) A corresponding oval circumscribed, mixed echogenicity mass is seen in the left breast at 1 o'clock position on ultrasound (thick arrow). (c) The left breast mass is hypermetabolic on ^{18}F-fluorodeoxyglucose positron emission tomography/computed tomography with no extramammary hypermetabolic foci (arrowhead). (d) High-power view (×400) of the breast mass biopsy with haematoxylin and eosin stain showing fibroadipose tissue infiltrated by sheets of medium- to large-sized neoplastic lymphoid cells. They possess irregular nuclear outlines, occasional nucleoli, and frequent apoptotic figures. On immunostaining (×40), the neoplastic lymphoid cells are diffusely positive for the B-cell marker CD20 (e) and negative for the T-cell marker CD3 (which highlights T lymphocytes in the background) [f]. Image courtesy of Dr Tiffany HT Chan and Dr HL Li, Department of Clinical Pathology, Pamela Youde Nethersole Eastern Hospital, Hong Kong (d-f).

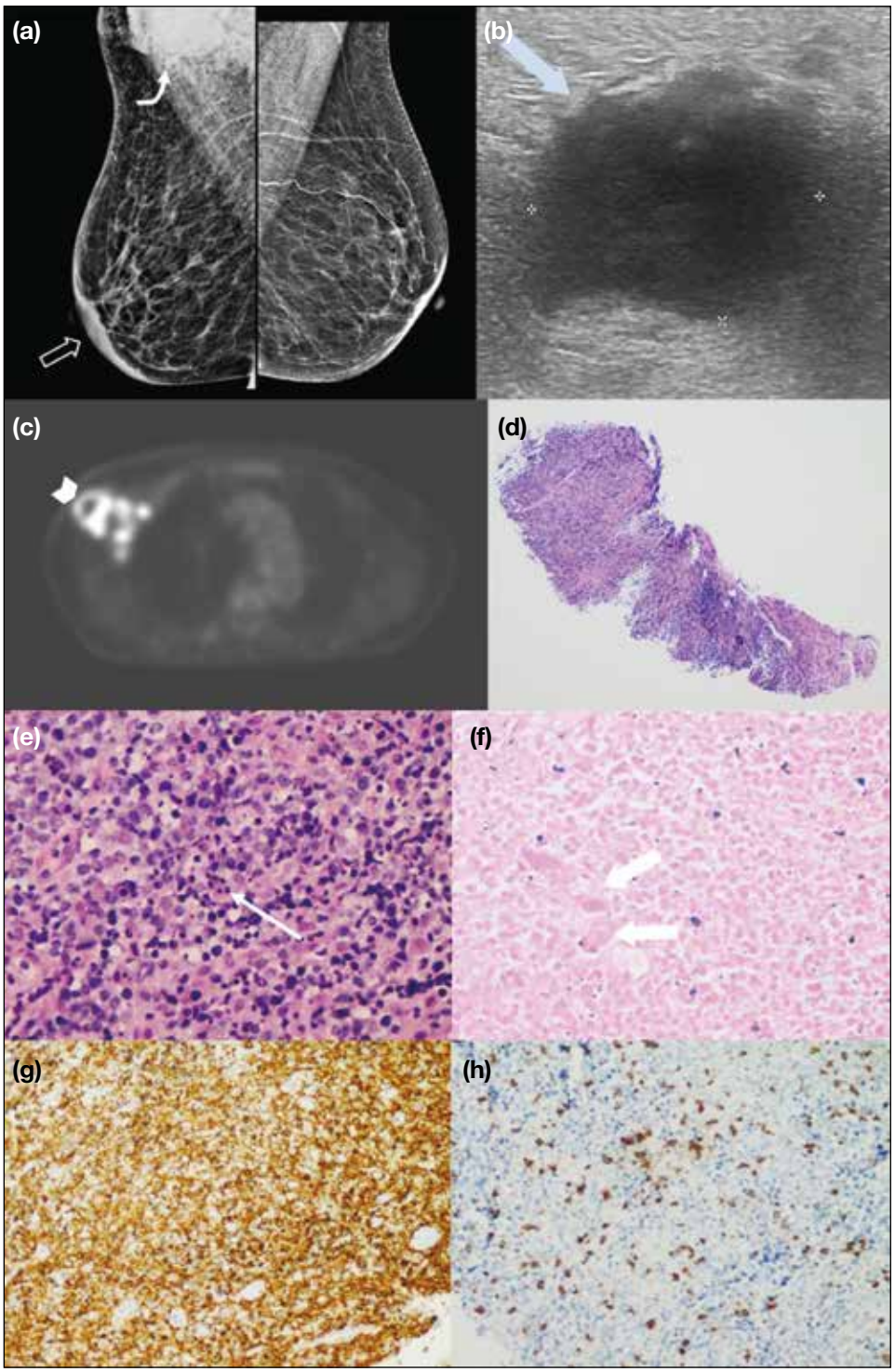

Figure 5. A 74-year-old woman presented with a right axillary mass. (a) Diffuse skin thickening and oedema (open arrow) of the right breast and axillary region were seen on bilateral mammograms in mediolateral oblique view. An enlarged right axillary lymph node (curved arrow) was also noted. (b) Ultrasound of the right axilla confirms the presence of enlarged irregular hypoechoic lymph nodes with loss of fatty hila (blue arrow). (c) The right axillary mass (arrowhead) demonstrates hypermetabolism on ^{18}F-fluorodeoxyglucose positron emission tomography/computed tomography, with multiple other sites of nodal involvement. (d) Histology sections with haematoxylin and eosin (H&E) stain in low-power view (×40) reveals the viable areas of the tumour as hypercellular. (e) High-power view (H&E staining, ×400) of the viable area showing sheets of medium- to large-sized neoplastic lymphoid cells with mitotic and apoptotic figures (thin arrow). (f) High-power view (H&E staining, ×400) of the necrotic area showing ghost outlines of neoplastic cells (thick arrows). On immunostaining (×200), the neoplastic lymphoid cells are diffusely positive for CD20 (g) and negative for CD3 (h). Overall features are consistent with diffuse large B-cell lymphoma. Image courtesy of Dr CK Cheung and Dr F Hioe, Department of Clinical Pathology, Pamela Youde Nethersole Eastern Hospital, Hong Kong (d-h).

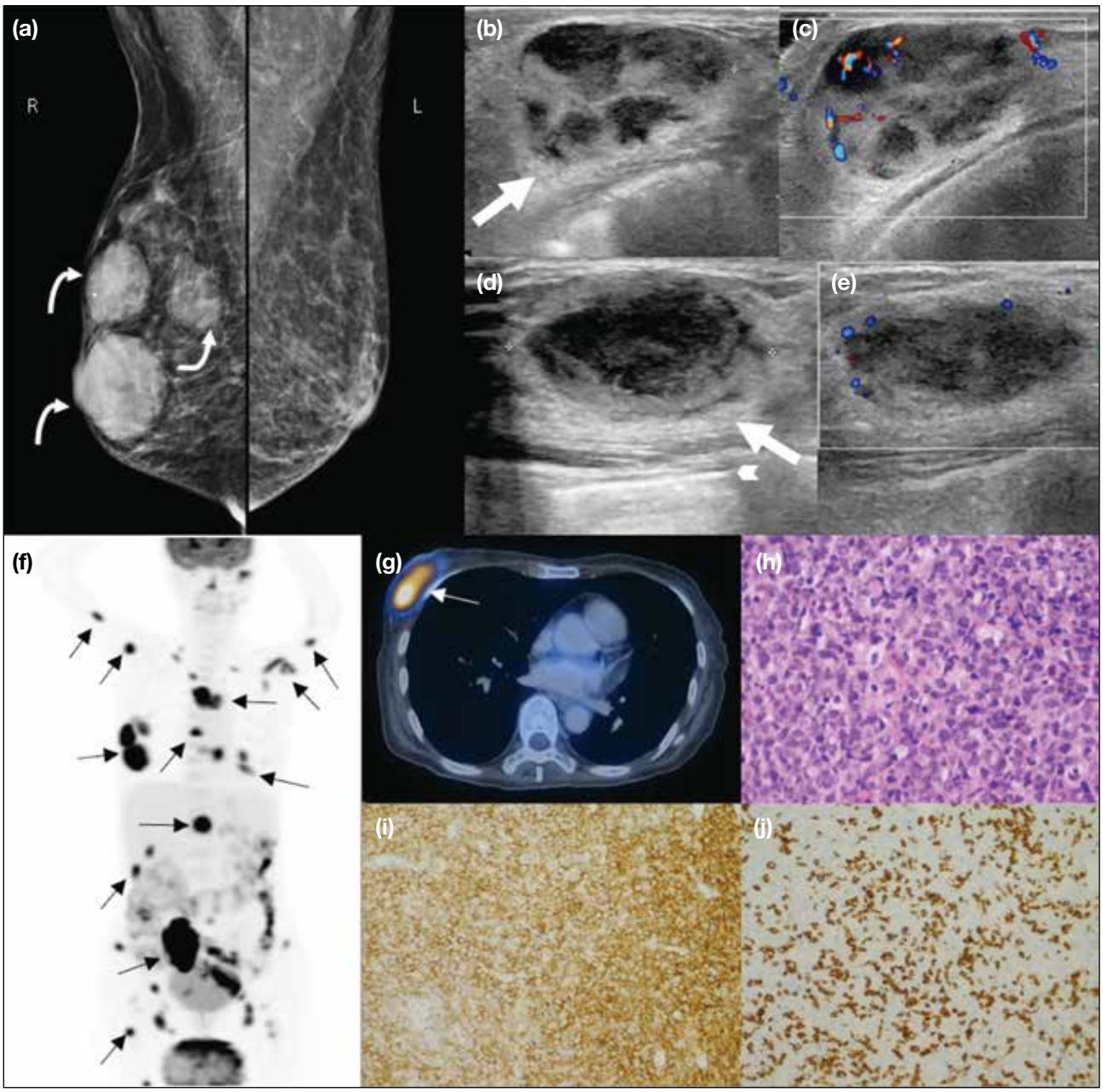

Figure 6. A 67-year-old woman with known history of stage IV follicular lymphoma with total metabolic response after chemotherapy presented with multiple new right breast lumps. (a) Bilateral mammograms showed three equal-density oval and circumscribed masses in the right breast without associated microcalcifications (curved arrows). (b-e) Multiple oval and circumscribed heterogeneous hypoechoic lesions were seen in the right breast, some with echogenic rims (thick arrows in [b] and [d]) and posterior enhancement (arrowhead in [d]). Internal vascularity is also visible in some of these lesions. (b, c) The first mass. Vascularity of this mass using Doppler ultrasound is shown in (c). (d) The second mass. The third mass with vascularity using Doppler ultrasound is shown in (e). (f, g) ^{18}F-fluorodeoxyglucose positron emission tomography/computed tomography images demonstrating extensive hypermetabolic disease involving the right breast (g) and multiple organs and systems (f) [black and white thin arrows]. (h) High-power view (×400) of the breast masses biopsy with haematoxylin and eosin stain showing diffuse sheets of neoplastic lymphoid infiltrate comprising medium- to large-sized cells with irregular nuclear membranes, hyperchromatic nuclei, and occasional nucleoli. Mitotic figures and apoptotic bodies are noted. On immunostaining (×200), the neoplastic lymphoid cells were diffusely positive for CD20 (i) and negative for CD3 (j). Overall features are consistent with diffuse large B-cell lymphoma. Image courtesy of Dr Elaine Lee, Department of Diagnostic Radiology, The University of Hong Kong (f, g); Dr CK Cheung and Dr MW Ma, Department of Clinical Pathology, Pamela Youde Nethersole Eastern Hospital, Hong Kong (h-j).

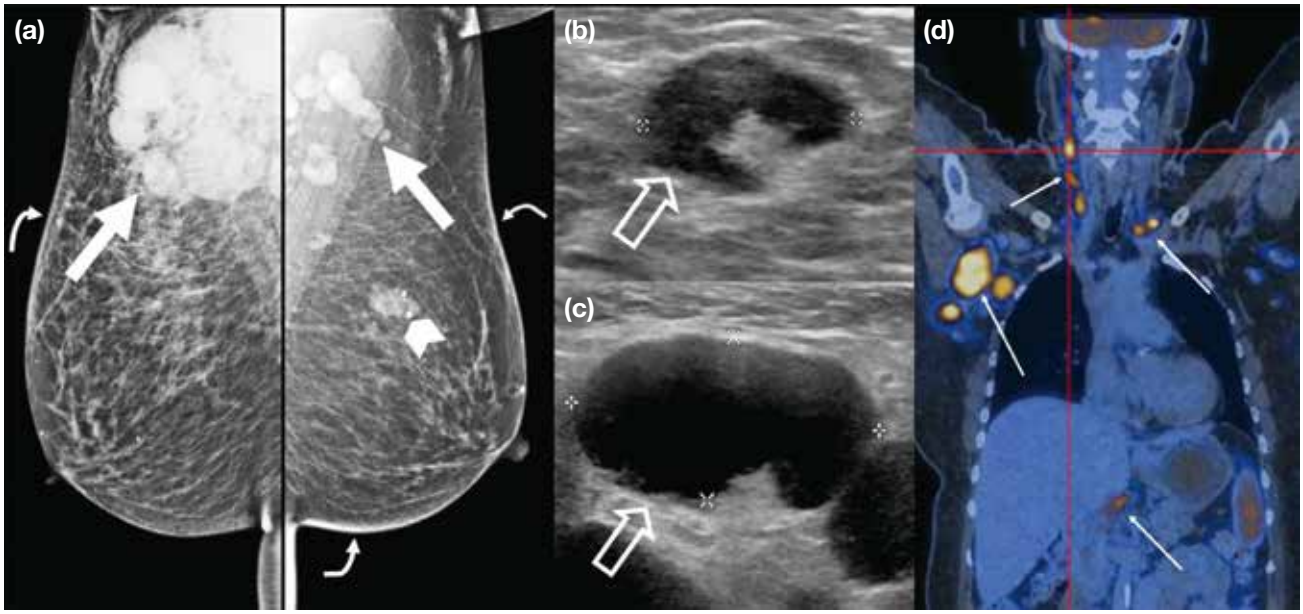

Figure 7. A 64-year-old woman presented with a right axillary mass. (a) Multiple bilateral enlarged axillary lymph nodes (thick arrows) and mild bilateral skin thickening (curved arrows) over both breasts are seen on bilateral mammograms. The mass with popcorn calcification in the left breast upper portion central depth (arrowhead) was a biopsy-proven fibroadenoma. (b, c) Ultrasound confirms the presence of multiple bilateral enlarged axillary lymph nodes with cortical thickening and loss of fatty hila (open arrows). (d) ^{18}F-fluorodeoxyglucose positron emission tomography/computed tomography showed multiple hypermetabolic lymphadenopathies above and below the diaphragm (thin arrows), including both axillae. Histopathology of the right axillary lymph node confirmed classical Hodgkin lymphoma.

hypo-, or mixed echogenicity, with circumscribed to indistinct margins (Figure 4).[12,15] Posterior acoustic enhancement, echogenic rims, and onion-peel–like rims are common findings (Figure 6).[14] Masses typically appear hypervascular on Doppler ultrasound.[12,17] Axillary lymphadenopathy has been reported in up to 32% of patients (Figures 5 and 7).[17]

The overall preponderance of breast lymphomas are diffuse large B-cell lymphomas,[18,19] which typically show ^{18}F-fluorodeoxyglucose (^{18}F-FDG) avidity on ^{18}F-FDG positron emission tomography/computed tomography (^{18}F-FDG PET/CT).[20] ^{18}F-FDG PET/CT is recommended for staging and response assessment of ^{18}F-FDG–avid lymphomas[21]; its role in the management of breast lymphoma has also been suggested.[22]

No specific imaging features can reliably distinguish between primary and secondary breast lymphoma. In patients with known extramammary lymphoma, multiple masses or an inflammatory-like appearance such as trabecular and skin thickening without a mass are more likely to suggest secondary breast lymphoma.[15,17]

PLASMACYTOMA

Plasmacytomas are tumours characterised by neoplastic monoclonal plasma cells in the bone or soft tissue (extramedullary). Extramedullary breast plasmacytomas are extremely rare and most commonly occur as a secondary event in patients with known multiple myeloma.[23] Clinically, breast plasmacytomas present as palpable lumps.

A retrospective study involving 53 cases of breast plasmacytoma examined its radiological features.[23] On mammography, they had a non-specific appearance, with dense, round, or oval masses with well- or ill-defined margins (Figure 8[24]), or as diffuse infiltration. On ultrasound, they can appear hypoechoic with well-defined margins but, less commonly, may display mixed hypo- to hyperechogenicity with indistinct margins and posterior acoustic enhancement or shadowing (Figure 8). No differentiating radiological features were found for primary and secondary breast plasmacytoma. Given the non-specific radiological features, the diagnosis of breast plasmacytoma relies on clinical suspicion when there is a history of multiple myeloma, and confirmation through histopathology.[23]

There are only a few reports on the magnetic resonance imaging features of breast plasmacytoma. Variable T1 and T2 signal intensities have been reported, including

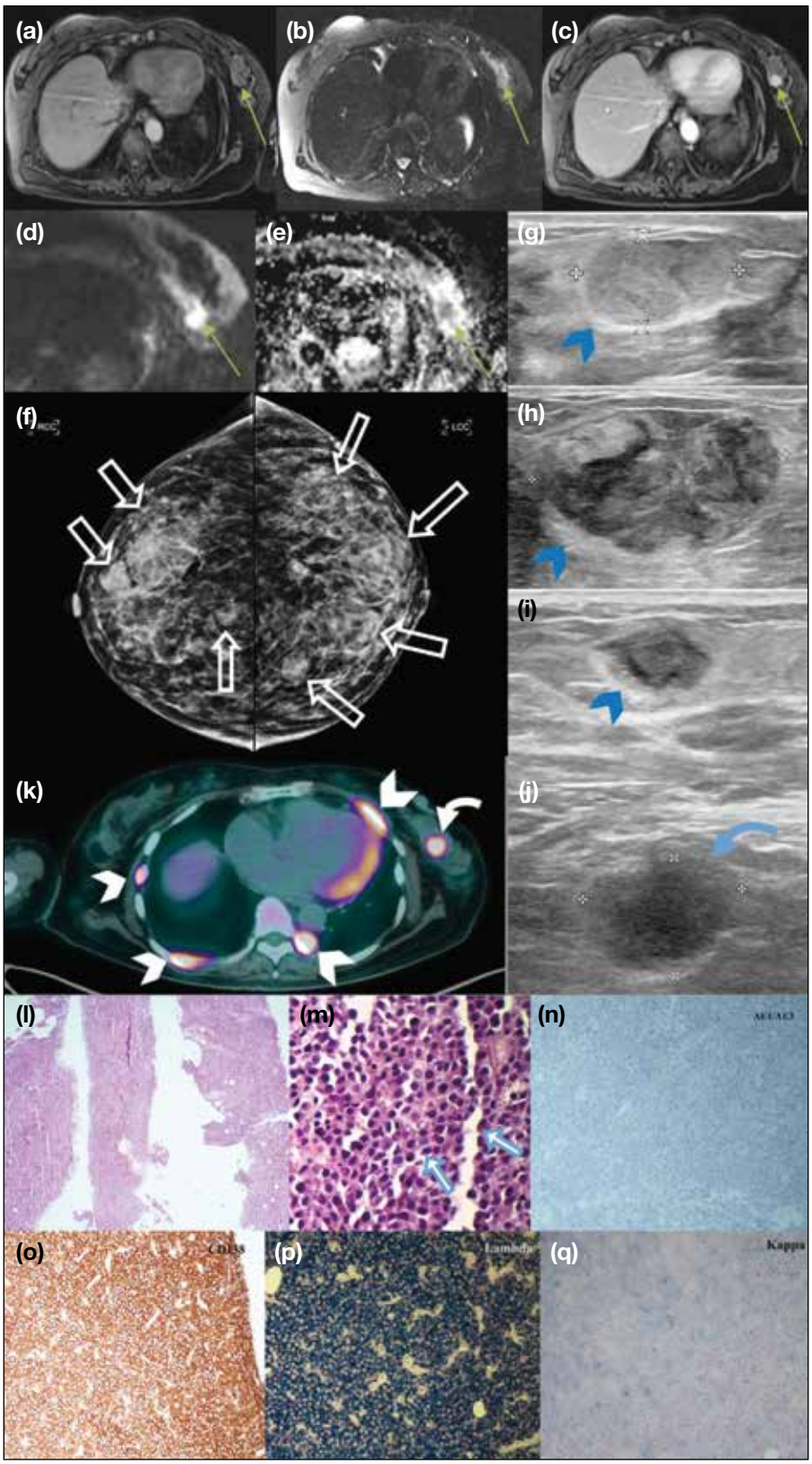

Figure 8. A 59-year-old woman with a known history of multiple myeloma was incidentally found to have a left breast lesion (thin arrows in [a] to [e]) in a contrast-enhanced magnetic resonance imaging study of the liver. The nodule is (a) isointense on the pre-contrast T1-weighted axial image, (b) hyperintense on the T2-weighted fat-saturated axial image, and (c) contrast-enhanced on the post-contrast T1-weighted axial image. Cropped images focusing on the lesion in the (d) diffusion-weighted imaging and (e) apparent diffusion coefficient sequences demonstrate restricted diffusion. (f) Further evaluation with bilateral mammography showing multiple equal- to high-density oval and irregular masses with circumscribed to ill-defined margins (white open arrows). (g-i) Ultrasound of both breasts showing multiple oval circumscribed masses corresponding to the mammographically detected lesions (blue arrowheads). The masses are of variable echogenicity, ranging from hyperechoic, mixed heterogeneous to hypoechoic. (j) A suspicious irregular hypoechoic left axillary lymph node with loss of fatty hilum is also seen (blue curved arrow). (k) Dual-tracer ^{18}F-fluorodeoxyglucose/^{11}C-acetate positron emission tomography/computed tomography showing hypermetabolism in the bilateral breast masses (white curved arrow); left axillary lymph nodes; and multiple other lesions in the liver, abdominal cavity, subcutaneous tissue, and skeleton (white arrowheads), suggestive of multiple myeloma with extraosseous involvement. (l) Histology sections with haematoxylin and eosin stain in low-power view (×40) showing sheets of tumour cells. (m) High-power view (×400) showing tumour cells possessing eosinophilic cytoplasm with perinuclear hof (blue and white arrows) and hyperchromatic nuclei. Immunohistochemically (×200), the tumour cells are negative for epithelial marker AE1/AE3 (pancytokeratin) [n] and positive for plasma cell marker CD138 (o). In situ hybridisation (×200) for lambda (p) and kappa (q) showing lambda light chain restriction. Overall features are consistent with plasmacytoma. Reproduced and adapted with permission from the Hong Kong Academy of Medicine (a-f, k, n, and o)[24]; image courtesy of Dr TS Wong and Dr KC Leung, Department of Clinical Pathology, Pamela Youde Nethersole Eastern Hospital, Hong Kong (l-q).

low-to-isointense signal on T1-weighted images and intermediate-to-high signal on T2-weighted images (Figure 8[24]).[25,27] Restricted diffusion and homogenous enhancement with delayed washout kinetics have also been noted (Figure 8[24]).[25-27]

A limited number of studies have reported on ^{18}F-FDG PET/CT findings in breast plasmacytoma.[26-29] Majority of these cases showed ^{18}F-FDG avidity,[26,27,29] although low-grade uptake has also been reported.[28] Nevertheless, ^{18}F-FDG PET/CT is increasingly being recognised as a valuable tool for the diagnosis and management of patients with plasma cell disorders, such as multiple myeloma and solitary plasmacytoma.[30] Several tracers other than ^{18}F-FDG for PET/CT have also been investigated in patients with multiple myeloma.[30]

CONCLUSION

Although non-epithelial malignancies of the breast show features different from those of epithelial breast carcinoma, in general their radiological appearance is generally variable and non-specific. Radiologists must interpret the imaging findings in conjunction with the clinical context. Biopsy remains the mainstay of diagnosis and should be considered in suspected cases.

REFERENCES

1. Feder JM, de Paredes ES, Hogge JP, Wilken JJ. Unusual breast lesions: radiologic-pathologic correlation. Radiographics. 1999;19 Spec No:S11-26.
2. Lee SH, Park JM, Kook SH, Han BK, Moon WK. Metastatic tumors to the breast: mammographic and ultrasonographic findings. J Ultrasound Med. 2000;19:257-62.
3. Toombs BD, Kalisher L. Metastatic disease to the breast: clinical, pathologic, and radiographic features. AJR Am J Roentgenol. 1977;129:673-6.
4. Bartella L, Kaye J, Perry NM, Malhotra A, Evans D, Ryan D, et al. Metastases to the breast revisited: radiological-histopathological correlation. Clin Radiol. 2003;58:524-31.
5. Krishnan EU, Phillips AK, Randell A, Taylor B, Garg SK. Bilateral metastatic inflammatory carcinoma in the breast from primary ovarian cancer. Obstet Gynecol. 1980;55(3 Suppl):94S-96S.
6. Vergier B, Trojani M, de Mascarel I, Coindre JM, Le Treut A. Metastases to the breast: differential diagnosis from primary breast carcinoma. J Surg Oncol. 1991;48:112-6.
7. WHO Classification of Tumours Editorial Board. WHO Classification of Breast Tumours: WHO Classification of Tumours, 5th Edition. World Health Organization; 2019. pp 261-5.
8. Lim SZ, Ong KW, Tan BK, Selvarajan S, Tan PH. Sarcoma of the breast: an update on a rare entity. J Clin Pathol. 2016;69:373-81.
9. Bousquet G, Confavreux C, Magné N, de Lara CT, Poortmans P, Senkus E, et al. Outcome and prognostic factors in breast sarcoma: a multicenter study from the rare cancer network. Radiother Oncol. 2007;85:355-61.
10. Matsumoto RA, Hsieh SJ, Chala LF, de Mello GG, de Barros N. Sarcomas of the breast: findings on mammography, ultrasound, and magnetic resonance imaging. Radiol Bras. 2018;51:401-6.
11. Smith TB, Gilcrease MZ, Santiago L, Hunt KK, Yang WT. Imaging features of primary breast sarcoma. AJR Am J Roentgenol. 2012;198:W386-93.
12. Berg WA, Leung JW. Diagnostic Imaging: Breast (3rd Edition). Philadelphia: Elsevier Health Sciences; 2019. pp 730-5.
13. Yang WT, Hennessy BT, Dryden MJ, Valero V, Hunt KK, Krishnamurthy S. Mammary angiosarcomas: imaging findings in 24 patients. Radiology. 2007;242:725-34.
14. Shim E, Song SE, Seo BK, Kim YS, Son GS. Lymphoma affecting the breast: a pictorial review of multimodal imaging findings. J Breast Cancer. 2013;16:254-65.
15. Raj SD, Shurafa M, Shah Z, Raj KM, Fishman MD, Dialani VM. Primary and secondary breast lymphoma: clinical, pathologic, and multimodality imaging review. Radiographics. 2019;39:610-25.
16. Surov A, Holzhausen HJ, Wienke A, Schmidt J, Thomssen C, Arnold D, et al. Primary and secondary breast lymphoma: prevalence, clinical signs and radiological features. Br J Radiol. 2012;85:e195-205.
17. Yang WT, Lane DL, Le-Petross HT, Abruzzo LV, Macapinlac HA. Breast lymphoma: imaging findings of 32 tumors in 27 patients. Radiology. 2007;245:692-702.
18. Au W, Chan AC, Chow LW, Liang R. Lymphoma of the breast in Hong Kong Chinese. Hematol Oncol. 1997;15:33-8.
19. Picasso R, Tagliafico A, Calabrese M, Martinoli C, Pistoia F, Rossi A, et al. Primary and secondary breast lymphoma: focus on epidemiology and imaging features. Pathol Oncol Res. 2020;26:1483-8.
20. Weiler-Sagie M, Bushelev O, Epelbaum R, Dann EJ, Haim N, Avivi I, et al. ^{18}F-FDG avidity in lymphoma readdressed: a study of 766 patients. J Nucl Med. 2010;51:25-30.
21. Cheson BD, Fisher RI, Barrington SF, Cavalli F, Schwartz LH, Zucca E, et al. Recommendations for initial evaluation, staging, and response assessment of Hodgkin and non-Hodgkin lymphoma: the Lugano classification. J Clin Oncol. 2014;32:3059-68.
22. Santra A, Kumar R, Reddy R, Halanaik D, Kumar R, Bal CS, et al. FDG PET-CT in the management of primary breast lymphoma. Clin Nucl Med. 2009;34:848-53.
23. Surov A, Holzhausen HJ, Ruschke K, Arnold D, Spielmann RP. Breast plasmacytoma. Acta Radiol 2010;51:498-504.
24. Mo CK, Lai AY, Lo SS, Wong TS, Wong WW. Bilateral breast multiple myeloma: a case report. Hong Kong Med J. 2022;28:488-90.
25. Neuhaus T, Hess T. Bilateral extramedullary plasmacytoma of the breast. Breast J. 2014;20:315-8.
26. Park YM. Imaging findings of plasmacytoma of both breasts as a preceding manifestation of multiple myeloma. Case Rep Med. 2016;2016:6595610.
27. Vong S, Navarro SM, Darrow M, Aminololama-Shakeri S. Extramedullary plasmacytoma of the breast in a patient with multiple myeloma. J Radiol Case Rep. 2020;14:14-23.
28. Ginat DT, Puri S. FDG PET/CT manifestations of hematopoietic malignancies of the breast. Acad Radiol. 2010;17:1026-30.
29. Rachh S, Puj K, Parikh A. ^{18}F-FDG PET/CT in the evaluation of solitary extramedullary plasmacytoma: a case series. Asia Ocean J Nucl Med Biol. 2021;9:56-61.
30. Cavo M, Terpos E, Nanni C, Moreau P, Lentzsch S, Zweegman S, et al. Role of ^{18}F-FDG PET/CT in the diagnosis and management of multiple myeloma and other plasma cell disorders: a consensus statement by the International Myeloma Working Group. Lancet Oncol. 2017;18:e206-17.